1 **Regulation of balanced root fungal community of *Vanda falcata* (Orchidaceae) by**

2 **partitioning its mycorrhizal fungi and ascomycetous fungi across growth and**

3 **development**

4

5 **Running title**: *Vanda-Ceratobasidium* association

6

7 Galih Chersy Pujasatria[1], Ikuo Nishiguchi[2], Chihiro Miura[3], Masahide Yamato[4], and Hironori

8 Kaminaka[3, *]

9

10 [1] The United Graduate School of Agricultural Science, Tottori University, Tottori 680-8553,

11 Japan

12 [2] Suzuka city, Mie 510-0226, Japan

13 [3] Faculty of Agriculture, Tottori University, Tottori 680-8553, Japan

14 [4] Faculty of Education, Chiba University, Chiba 263-8522, Japan

15

16 [*] Corresponding author

17

18 **Corresponding Author:**

19 Hironori Kaminaka

20 　Tel: +81-857-31-5378

21 　E-mail: kaminaka@tottori-u.ac.jp

22

23   **ORCID**

24   Galih Chersy Pujasatria: https://orcid.org/0000-0002-2768-8250

25   Masahide Yamato: https://orcid.org/0000-0003-2238-4044

26   Hironori Kaminaka: https://orcid.org/0000-0002-3685-8688

27

28

Abstract

Epiphytic orchids are commonly found in exposed environments, which plausibly lead to different root fungal community structures from terrestrial orchids. Until recently, no studies have been conducted to show the fungal community structure during the growth of a photosynthetic and epiphytic orchid in its natural growing state. In this study, the *Vanda falcata* (commonly known as *Neofinetia falcata*)*,* one of Japan's ornamental orchids, was used to characterize the fungal community structure at different developmental stages. Amplicon sequencing analysis showed that all development stages contain a similar fungal community: Ascomycota dominates half of the community while one-third of the community is Basidiomycota. *Rhizoctonia*-like fungi, a term to group the most common basidiomycetous fungi that form orchid mycorrhiza, exist even in a smaller portion (around a quarter) compared to other Basidiomycota members. While ascomycetous fungi exhibit pathogenicity, two *Ceratobasidium* strains isolated from young and adult plants could initiate seed germination *in vitro*. It was also found that the colonization of mycorrhizal fungi was concentrated in the lower part of the root where it directly attaches to the phorophyte bark, while ascomycetous fungi were distributed in the velamen but never colonized cortical cells. Additionally, lower root parts attached to the bark have denser exodermal passage cells, and these cells were colonized only by mycorrhizal fungi that further infiltrated the cortical area. Therefore, we propose that physical regulation of fungal entry to partition the ascomycetes and mycorrhizal fungi results in the balanced mycorrhizal symbiosis in this orchid.

(243 words)

Keywords: *Ceratobasidium*, epiphytic orchid*,* fungal microbiome*,* microbial dynamics, symbiotic germination, *Vanda falcata*

Introduction

54 Orchidaceae, one of the biggest flowering plant families, is widely distributed in almost all

55 parts of the world. However, many orchid species are listed as endangered owing to habitat

56 degradation and dependence on other organisms, i.e., pollinators (Suetsugu et al. 2015; Freitas

57 et al. 2020). Moreover, establishing orchids in the natural habitat is always complicated, even

58 in suitable conditions (Pujasatria et al. 2020). Due to its unique, one-of-a-kind traits, orchid

59 seed germination is often hard to occur naturally. Despite extremely high fecundity,

60 endosperm in orchids' seeds is almost absent. Consequently, orchids' seeds are nearly

61 impossible to germinate without nutritional support. For seeds to successfully germinate and

62 grow into mature plants, they must establish orchid mycorrhizal (OM) symbiosis (Arditti and

63 Ghani 2000; Barthlott et al. 2014; Yeh et al. 2019; Pujasatria et al. 2020). Colonization of

64 orchid mycorrhizal fungi (OMF) starts at seed germination and may last until adulthood. As

65 with other mycorrhizae, OMF forms coiled hyphae in its host cells. This structure is termed

66 peloton, where the exchange of nutrients (e.g., carbon, nitrogen, and phosphorus) occurs (Yeh

67 et al. 2019). However, OM is unique because the host eventually digests the pelotons for

68 further nutrient acquisition (Kuga et al. 2014). Based on this, orchids are considered

69 parasitizing the fungus. This behavior, termed mycoheterotrophy, occurs mostly during the

70 early growth stage where protocorms are still achlorophyllous and may continue until

71 adulthood in various genera (Rasmussen et al. 2015; Yeh et al. 2019).

72 Most orchids associate with *Rhizoctonia*-like fungi, a broad term for several genera

73 resembling the anamorphic morphology of *Rhizoctonia*. As symbionts, there are three

74 genera in this group: *Ceratobasidium, Serendipita* (often associated with *Sebacina sensu*

75 *lato*), and *Tulasnella* (Rasmussen et al. 2015; Yeh et al. 2019; Pujasatria et al. 2020).

76 Originally, those fungi are saprophytic, endophytic, or even pathogenic. However, among

4

77   those genera, many species were isolated from orchid roots and proved to be mycorrhizal

78   upon co-inoculation with seeds of respective orchid species (Pujasatria et al. 2020).

79   Studies on OMF of epiphytic orchids are lacking despite their vast diversity, compared to

80   terrestrial orchids (Yukawa et al. 2009). While the roots of terrestrial orchids are usually

81   subterranean, epiphytic orchids are commonly found growing in exposed environments and

82   are prone to desiccation due to weather change (Rachanarin et al. 2018; Freitas et al. 2020).

83   This leads to a presumably different fungal community compared to those of the underground.

84   Microclimate change and phorophyte architecture also affect the establishment of epiphytic

85   orchids (Rasmussen and Rasmussen 2018), especially for those living in a fluctuating climate,

86   such as temperate regions. The availability of OMF on a particular substrate–in this case,

87   arboreal–is also dependent on such a microenvironment since fungus intrinsically prefers

88   unexposed, moist conditions to grow. When orchid seed lands on the substrate, its

89   germination is not guaranteed since colonization of appropriate OMF is required. Thus, the

90   interaction between 'the orchid and the fungal community would be important during the

91   orchid's establishment and growth.

92   Most epiphytic orchids studied tend to associate with either *Ceratobasidium* or *Tulasnella*

93   (Yukawa et al. 2009; Zettler et al. 2013; Rachanarin et al. 2018; Pujasatria et al. 2020; Freitas

94   et al. 2020). However, more specifically, studies on OMFs of monopodial epiphytic orchids

95   are limited. Several studies were already conducted on angraecoids (Hoang et al. 2017;

96   Kendon et al. 2020), either leafy or aphyllous, but still limited to vandaceous (Carlsward et al.

97   2006).

98   This study focused on *Vanda* (syn. *Neofinetia*) *falcata*. This epiphytic orchid is known as

99   one of Japan's ornamental orchids. Naturally, this orchid is distributed across central to

100   southern Japan and reportedly grows on evergreen or deciduous trees (Suetsugu et al. 2015).

101   Unlike typical epiphytic orchids concentrated in tropical regions, *V. falcata* is adapted to

102   subtropic and to the temperate areas, which may affect its association with fungi on

103   phorophytes. Previous studies suggested that vandaceous orchids–especially those of

104   subtribe Aeridinae–mainly associated with *Ceratobasidium*, proven by metabarcoding and

105   seed germination results (Otero et al. 2002; Yukawa et al. 2009; Hoang et al. 2017; Mújica

106   et al. 2018; Rammitsu et al. 2019; Kendon et al. 2020). Although *Ceratobasidium* strains

107   have also been isolated from *V. falcata* (Rammitsu et al. 2021)*, mycobionts for seed

108   germination have never been reported. Thus, this study analyzed the whole fungal

109   community in seeds and root samples of *V. falcata* using amplicon sequencing.

110   Additionally, pure fungal cultures were isolated from the same root pieces. Based on

111   microscopic and molecular analysis, it was found that some of the isolated fungi were

112   *Rhizoctonia*-like fungi. Finally, co-inoculation experiment was conducted to determine the

113   interaction of these fungi for their colonization with seeds and roots of *V. falcata*.

114

115   **Materials and Methods**

116   *Plant materials*

117   *Vanda falcata* plants growing on a persimmon (*Diospyros kaki*) trunk were obtained from

118   Kihoku Town, Mie Prefecture, Japan (34°06'27" N, 136°14'17" E). The residents eventually

119   cut the trunk due to safety reasons, and it was maintained in Suzuka City of the same

120   prefecture (34°51'05" N, 136°36'123" E) (Fig. 1A). Roots of young (small to medium plants

121   that never flowered) and adult (those already flowered at least once) plants (Fig. 1B, C)

122   attached to bark were randomly collected, and the harvested samples were stored at 4°C until

123   use. The baiting method assessed fungal diversity inside the seeds: 3 x 6 cm nylon mesh

124   packs containing ca. 100 *V. falcata* seeds were tied adjacent to twelve randomly selected

125   plants, including young and adult plants. The baiting method was conducted during spring

126   (March–June 2020). The seeds and young/adult plant roots were surface sterilized and stored

127   in 70% ethanol at 4°C until DNA extraction.

128

129   *DNA extraction from plant materials and amplicon sequencing*

130   Seeds isolated from the baiting method and root segments of randomly selected young and

131   adult plants were used as materials for DNA extraction using the Real Genomics Plant DNA

132   Extraction kit (RBC Bioscience, Taipei, Taiwan). After extraction, DNA concentration was

133   measured using DS-11 spectrophotometer (DeNovix, DW, USA). The internal transcribed

134   spacer (ITS) region was amplified using ITS1F_KYO1/ITS2_KYO2 for ITS1 and a pair of

135   gITS/ITS4 for ITS2 (Ihrmark et al. 2012; Toju et al. 2012) (Table S1). Each reaction mixture

136   (20-µl) contains 1-ng genomic DNA, 1-µl of 20-µM primer forward/reverse, and 10-µl KOD

137   One PCR Master Mix (Toyobo, Osaka, Japan). For amplification, PCR was coonducted on

138   T100 thermal cycler (Bio-Rad, CA, USA) using the following program: initial denaturation at

139   94°C for two minutes, 94°C for 30 secs, followed by 25 cycles of 50°C for 30 secs, 72°C for

140   one minute, and final elongation step at 72°C for seven minutes. PCR results were confirmed

141   using 1% (w/v) agarose gel electrophoresis. The sequencing of libraries prepared by PCR

142   with barcode-containing primers using Illumina MiSeq platform (2 × 300 bp) and data

143   analysis was conducted by the Bioengineering Lab Co., Ltd. (Atsugi, Japan). The raw

144   sequence data obtained as fastq file was processed using the FASTX toolkit v0.0.13 (Hannon

145   2010) and Sickle v1.33 (Joshi and Fass 2011) to remove adaptor and primer sequences,

146   ambiguous reads, low-quality sequences (quality score less than Q20), and reads no more than

147   40-bp. Quality-filtered sequences were merged using FLASH v1.12.11 (Magoč and Salzberg

148   2011) and used for the production of the representative sequences and operational taxonomic

149 unit (OTU) table using Qiime2 (v2020.6) (Bolyen et al. 2019) after removing the illusion and

150 noise sequences using dada2 plugin. The representative sequences were compared to OTUs

151 (97%) in UNITE v8.2 (Nilsson et al. 2019) to classify by taxon using the fitted classifier of

152 Qiime2. Additionally, alpha and beta diversity analyses were conducted using Qiime2

153 diversity plugin.

154 Amplicon sequencing results were visualized using RStudio v4.0.2. The *ggpubr* package

155 was used to visualize fungal diversity indices (OTU abundance, Chao1, Pielou, and

156 Shannon Evenness Index/SEI), and the proportion of each fungal phylum observed in

157 samples (Kassambara 2018). Principal coordinate analysis (PCoA) plots–based on Bray-

158 Curtis index, Euclidean distance, and without any data transformations–were visualized

159 using the *vegan* package (Oksanen et al. 2007). Additionally, analysis of similarity

160 (ANOSIM) was used to calculate PCoA statistical significance ($p < 0.05$), using the same

161 package.

162

163 *Fungi-colonized root morphology observation*

164 Crossing manual sections of fungi-colonized root were stained using 3% (w/v) acid fuchsin in

165 glacial acetic acid (Gange et al. 1999) or UV autofluorescence after clearing in 10% KOH for

166 one hour at 90°C to observe the presence of OMF and other fungi. The samples were then

167 observed under a light microscope (BX53; Olympus, Tokyo, Japan), and images were taken

168 using the equipped digital camera (DP27; Olympus). Statistics for quantification of OMF

169 colonization in roots was calculated using ANOVA based on the results of the Kolmogorov-

170 Smirnov normality test and Bartlett test using *ggpubr* package of RStudio v4.0.2 (Kassambara

171 2018). Subsequent Tukey *post hoc* test was conducted using the same software.

172

8

173   *Rhizoctonia-like and pathogenic fungi isolation*

174   Roots of young and adult plants were sectioned manually and observed using light (BX53) or

175   stereo microscope (SZX16; Olympus). Subsequently, root sections with fungal colonization in

176   cortex were put on either potato dextrose agar (PDA), one-sixth strength Czapek-Dox agar, or

177   Fungal Isolation Medium (Zettler et al. 2013) supplemented with 10-µg/mL tetracycline.

178   Fungi with *Rhizoctonia*-like characteristics (Oberwinkler et al. 2013; Weiß et al. 2016) were

179   cultured on PDA, malt extract agar (MA), full-strength V8 juice agar (V8), or oatmeal agar

180   (OMA) media at 25°C, and then stored at 4°C for long-term storage, while all non-

181   *Rhizoctonia*-like fungi were cultured only on OMA at 25°C. Hyphae were stained using

182   0.01% ethidium bromide in 25% ethanol (Singh and Kumar 1991), and the cell wall was

183   stained using a mixture of 1-mg/L calcofluor white and 0.5-mg/L Evans blue, to count the

184   nuclei of *Rhizoctonia*-like fungal hyphae. Samples were observed under a fluorescence

185   microscope (DM2500; Leica, Wetzlar, Germany) equipped with a digital camera (DFC310

186   FX; Leica) and visualized using ImageJ v.1.53a.

187   Fungal genomic DNA was extracted from the cultured fungi using the sorbitol-

188   cetrimonium bromide (CTAB) combination method (Inglis et al. 2018). After extraction,

189   DNA concentration was measured as described above. The ITS region was amplified using a

190   combination of ITS1OF/ITS4 (Table S1) (Taylor and McCormick 2008; Toju et al. 2012).

191   The PCR mixture for each sample contains 1-µl fungal genomic DNA, 1-µl of 20-µM primer

192   forward/reverse, and 10-µl GoTaq Green Master Mix (Promega, WI, USA). Amplification

193   was conducted using the following program: initial denaturation at 95°C for ten minutes,

194   followed by 35 cycles at 95°C for 20 secs, 50°C for 30 secs, 72°C for 20 secs, and a final

195   elongation step at 72°C for seven minutes. Successfully amplified DNA fragments confirmed

196   by 1% (w/v) agarose gel electrophoresis were cloned using TOPO TA Cloning Kit

197 (ThermoFischer Scientific, MA, USA) and sequenced using Sanger method with both M13

198 forward and reverse primers by Eurofins Genomics (Tokyo, Japan). DNA sequences were

199 subjected to BLAST (https://blast.ncbi.nlm.nih.gov/Blast.cgi) to identify the closest taxa.

200

201 *Phylogenetic analysis*

202 Fungal ITS DNA sequences were aligned using ClustalW v1.6, and subsequent maximum

203 likelihood (ML) phylogenetic tree construction was conducted using RAxML-HPC v8.2.10

204 implemented in GENETYX-Windows v15 (Genetyx, Tokyo, Japan) with GTRGAMMA

205 model and 1000 bootstrap analysis to infer the phylogenetic position of fungal OTUs and

206 isolated strains of *Rhizoctonia*-like fungi. The best rooted tree was visualized using Iroki

207 online tool (Moore et al. 2020).

208

209 *In vitro seed germination assay*

210 Eleven *Rhizoctonia*-like fungal strains containing *Ceratobasidium, Serendipita,* and

211 *Tulasnella* (Table 1), obtained from culture stock centers, ATCC (American Type Culture

212 Collection), RIKEN bioresource center (JCM strain), NARO Genebank (MAFF strains) and

213 NITE biological resource center (NBRC strains), were inoculated on OMA for two weeks

214 before symbiotic germination assay. Dehiscent capsules formed from naturally pollinated

215 flowers were used to obtain the *V. falcata* seeds. Seeds were sterilized using 3% hydrogen

216 peroxide and washed two to three times with sterilized water. Cultures were stored at 25°C for

217 eight weeks in darkness. Germination stage description (Zettler et al. 2007) was modified

218 according to the preliminary germination assay result (Table 2, Fig. S1). Protocorm growth

219 index (GI) was evaluated using the equation $GI = \sum_{i=5}^{n} i(S_i) / \sum S$, with i; germination stage

220 number (starting from stage 0 to 5), n; total seeds in one treatment, and n_i; total seeds

10

221   reaching germination stage *i* (Guimarães et al. 2013), and symbiotic cells were counted after

222   six weeks. Each fungal treatment was replicated four times, with each plate containing ca.

223   100–300 seeds. Additionally, two ascomycetous fungi isolated from roots, *Pyrenochaetopsis*

224   and *Fusarium,* were also subjected to similar germination assay to observe their interaction

225   with seeds (Table 3). Protocorms were stained using 1-g/L calcofluor white counterstained

226   with 0.5-g/L Evans blue, and fungal hyphae were stained using 1-mg/L WGA-Alexa Fluor

227   594 (ThermoFisher Scientific). Visualization was conducted using a fluorescent microscope

228   (DM2500) equipped with a digital camera (DFC310 FX) and ImageJ v.1.53a, while symbiotic

229   cells were counted using a tally counter from 25 randomly selected protocorms. Based on the

230   results of the Kolmogorov-Smirnov normality test and Bartlett test, the Kruskal–Wallis test

231   was conducted using *ggpubr* package of RStudio v4.0.2 (Kassambara 2018). Subsequently,

232   Dunn's *post hoc* test with Benjamini-Hochberg false discovery rate adjustment ($p < 0.05$) was

233   conducted using the *FSA* package of the same software (Ogle et al. 2021).

234

235   **Results**

236   *Amplicon sequencing*

237   Genomic DNA was obtained from three kinds of samples: seeds, roots of young plants, and

238   roots of adult plants. The seeds were taken from twelve seed packs and combined as one even

239   though no germinating seeds were found. For root samples, three to four root sections (ca. 5-

240   cm each) were cut from a young or adult plant. In root samples, the most conspicuous feature

241   of the symbiotic region was a yellowish root surface that contains digested pelotons (Fig. 1D).

242   This was primarily obvious when the roots were wet. This coloration is unique to the root

243   parts directly attached to *D. kaki* bark (Fig. 1E).

11

244   The ITS1 and ITS2 PCR products were subjected to amplicon sequencing by Illumina

245   MiSeq. Each sample sequencing generated 36,027 to 72,301 raw reads for ITS1 and 40,033 to

246   72,014 raw reads for ITS2. 83% and 89.47% of the whole reads were processed and used

247   for further analysis (Table S2). Phylogenetic OTUs were generated at 97% similarity cutoff

248   using Qiime2 and ranged from 155 to 411 OTUs for each sample in ITS1 and 174 to 476

249   OTUs for each sample in ITS2 (Table S3, S4). In total, 1274 and 1358 phylogenetic OTUs

250   were obtained for ITS1 and ITS2, respectively.

251

252   *General fungal diversity and OMF localization in roots*

253   PCoA results conducted using generated OTUs from both ITS sequenced data showed distinct

254   groupings of fungal communities among the three development stages–seed, young plant, and

255   adult plant (Fig. 2), but ANOSIM did not give a significant result for ITS2 ($p < 0.05$). R-value

256   of 0.3913 (sig. = 0.0419) for ITS1 and 0.2047 (sig. = 0.1965) for ITS2 shows that the fungal

257   compositions between the stages were not distinguished (Clarke 1993) (Fig. 2). R-value

258   between ITS1 and ITS2 communities has different significance level but both values imply

259   that the degree of discrimination is not changed. The community structure similarities were

260   also supported by Pielou evenness (J') and SEI, where fungal diversity in all samples was not

261   significantly different (Fig. S2). Ascomycota and Basidiomycota were the most prevalent

262   phyla at the phylum level, with coverage of above 50% in each sample (Fig. S3). The other

263   phyla were Chytridiomycota, Mortierellomycota, and Mucoromycota, which were found in

264   smaller amounts.

265   In *Rhizoctonia*-like fungi, *Ceratobasidium* was found in trace amounts in seed samples

266   but was unexpectedly found only in one young root sample. It was also found in two other

267   adult root samples but only in trace amounts. Another similar case is in *Serendipita*, which

12

268 was relatively abundant only in seed samples. *Tulasnella* was very limited in seed samples but

269 gradually increased in young and adult root samples (Fig. 3A, S4). Thus, while the whole

270 fungal community did not alter, existence of *Rhizoctonia*-like fungi (*Ceratobasidium,*

271 *Serendipita,* and *Tulasnella*) tended to change over time following the growth and

272 development of *V. falcata.*

273   Both ITS sequences exhibited relatively similar diversity indices. However, ITS2 has been

274 considered a suitable marker for revealing the operational taxonomic richness and taxonomy

275 specifics of fungal communities due to the broader taxonomic information (Yang et al. 2018).

276 Therefore, this study mainly focused on the ITS2 sequences in subsequent analysis.

277

278 *Identification of Rhizoctonia-like fungal OTUs*

279 Among all basidiomycetous fungal sequences, fourteen OTUs annotated as Rhizoctonia-like

280 genera (Table S5) were extracted for the heatmap diagram (Fig. 3A). ML phylogenetic trees

281 based on the representative sequences of each OTU were constructed to see whether the fungi

282 belong to a particular OMF species in their respective families (Fig. 3B). Five

283 *Ceratobasidium* OTUs (accession numbers LC602782–LC602785) were closely related to a

284 mycobiont of epiphytic orchid *Taeniophyllum glandulosum* isolated in Japan (LC405936)

285 (Rammitsu et al. 2019). Six *Serendipita* OTUs (LC602788–LC602792) assigned to

286 Sebacinaceae were divided into two clades inside Serendipitaceae: two OTUs were related to

287 *Serendipita herbamans* (NR144842), an endophyte of *Bistorta vivipara* (Polygonaceae)

288 (Riess et al. 2014) in one clade, and the other four OTUs were close to *S. indica* (NR166023,

289 KF061284, MH863568), a well-known endophyte occurring in several flowering plants

290 (Weiß et al. 2016). Two *Tulasnella* OTUs (LC602793 and LC602794) were related to *T.*

291 *irregularis* (EU218889) and *T. amonilioides* (JF907601 and JF907599), mycobionts first

13

292   reported in *Dendrobium affine* (syn. *dicuphum*) and *Encyclia dichroma*, respectively (Warcup

293   and Talbot 1980; Almeida et al. 2014).

294

295   *Isolation of Rhizoctonia-like fungi from plant samples*

296   We initially attempted to isolate pure fungal cultures from all samples (seeds, protocorms, and

297   roots) to verify that *V. falcata* associated with *Rhizoctonia*-like fungus during the

298   development *in situ*. However, since no germinating seeds were found, roots of randomly

299   selected young and adult plants were only used for the fungal isolation. We could only isolate

300   two pure isolates of *Rhizoctonia*-like fungi from these root sections despite more than 30

301   attempts, including those with conspicuous symbiotic regions. We faced two major challenges

302   to obtain a pure culture, which include: (1) most pelotons were already digested, and (2) other

303   endophytic ascomycetous fungi–mostly those morphologically resembling *Trichoderma*,

304   *Cladosporium*, or *Phoma*–often outgrew preferred *Rhizoctonia*-like fungi in the isolation

305   media. In root samples, ascomycetous fungi were found in the epidermis with its conidial

306   form (Fig. 4A). Based on the conidia structure, some of these fungi were identified as

307   *Lasiodiplodia* and Pleosporales (Zhang et al. 2012). However, upon further examination into

308   exodermis, no fungi colonized the exodermal cells. Instead, *Rhizoctonia*-like fungi formed

309   peloton in exodermal passage cells. Based on hyphal morphology, it resembles *Rhizoctonia*-

310   like fungus isolated from roots: both possess hyphae with irregular width, commonly called

311   monilioid hyphae (Fig. 4B, S5). Upon forming peloton inside passage cells, the *Rhizoctonia*-

312   like fungi infiltrate cortical cells to form the peloton network. Additionally, passage cells are

313   concentrated in lower part of the root. Following this, OMF is also mostly found in the same

314   part (Fig. 4C).

14

315   The isolated *Rhizoctonia*-like fungi were named BI-103P from young and DE-52P

316   from the adult plant root segments (Table 3, Fig. S6A, B). Morphologically, those fungal

317   strains followed common descriptions for *Rhizoctonia*: branching at a right angle, constriction

318   of hyphae at the site of branching, occasionally visible dolipore septa, and septation at a short

319   distance after branching (Ogoshi 1975). The ITS sequences of these isolates were subjected to

320   pairwise DNA alignment, a feature of Mycobank (https://www.mycobank.org/) and BLAST,

321   which revealed that both strains belong to Ceratobasidiaceae. These strains were closest to

322   AB507066.1, an uncultured *Ceratobasidium* from another epiphytic orchid *Phalaenopsis* (syn.

323   *Sedirea*) *japonica* from Miyazaki Prefecture in southern Japan (Yukawa et al. 2009). We also

324   found that the hyphae are binucleate, indicating that these fungi are traditionally classified

325   into 'binucleate *Rhizoctonia'* (Fig. S6C, D).

326

327   *In vitro seed germination using isolated Ceratobasidium strains and Ascomycota fungi*

328   *V. falcata* seeds were used for symbiotic germination using isolated *Ceratobasidium* strains

329   and other *Rhizoctonia*-like fungi strains including *Serendipita* and *Tulasnella* obtained from

330   culture stock centers (Table 1). Seeds inoculated with compatible OMF started to undergo

331   imbibition and usually formed rhizoids upon entering stage 2 (Fig. S1A). Protocorms started

332   to turn greenish at the onset of stage 3, and shoot primordium was developed as an irregular

333   protrusion on the terminal part (Fig. S1B). This protrusion will eventually form a crest (Fig.

334   S1C). Compared to other stages, stage 4 protocorms were rarely observed. This stage is

335   characterized by the formation of the first leaf (Fig. S1C). Based on fluorescence imaging,

336   fungal colonization started from the suspensor and spread up to 75% of protocorm size (Fig.

337   S1D).

15

338   Based on the germination stage description summarized in Table 2, four of six

339   Ceratobasidium strains (C. sp. BI (BI-103P), C. sp. DE (DE-52P), C. sp. TA1, and C. sp.

340   TA2) yielded remarkably higher GI than others based on Kruskal-Wallis test ($p < 0.05$)

341   (Fig. 5A). Following GI, symbiotic cell count also increased. Protocorms yielded from

342   suitable fungal treatments also had a high symbiotic cell count (Fig. 5B). It was found that

343   these four strains are included in the same phylogenetic clade (Fig. 6). However, few

344   symbiotic cells were found in other Ceratobasidium, Serendipita, and Tulasnella treatments.

345   These strains could only induce germination until stage 1 even after eight weeks. The

346   protocorms kept swollen, but no pathogenic effect was observed, indicating that these

347   strains simply did not further associate with protocorms, and the swelling was merely a

348   result of imbibition. These results indicated that V. falcata seeds may have specificity

349   toward a group of Ceratobasidium fungi.

350   During the process of isolating the *Rhizoctonia*-like fungi from root samples, two

351   Ascomycota fungi *Pyrenochaetopsis* (NE-4) and *Fusarium* (MI-5) (Table 3), were also

352   isolated and identified. Since these are known as pathogenic fungi, the effects of these non-

353   *Rhizoctonia*-like fungi on *V. falcata* seeds were also analyzed using *in vitro* germination

354   assay. At the early stage, seeds were swelling and colonized by *Pyrenochaetopsis* but

355   eventually killed after pycnidia formation, indicated by the blackening of seeds (Fig. 7A).

356   Similarly, the seeds sown on *Fusarium* were heavily colonized and were eventually

357   degraded (Fig. 7B). These results suggested the importance of partitioning between

358   ascomycetous and *Rhizoctonia*-like fungi inside the roots. Additionally, these

359   ascomycetous fungi were incompatible with *V. falcata* seeds for germination.

360

361   **Discussion**

16

362   While most reports on mycorrhizal associations of the Vandeae tribe come from the

363   Angraecinae subtribe (angraecoids), reports on the Aeridinae subtribe members are still

364   minimal. This study focused on *V. falcata* fungal community structure of the three

365   developmental stages, i.e., seeds, young plants, and adult plants. This study emphasizes this

366   point to show how an orchid maintains its inner fungal community in each developmental

367   stage. All observations provided several findings. Firstly, Ascomycota was the dominant

368   phylum in all examined seeds, young plants, and adult plants. Secondly, ascomycetous, some

369   of which are potential pathogenic fungi, colonized epidermal areas of *V. falcata* roots, while

370   *Rhizoctonia*-like fungi (OMF) colonized the cortical area. Thirdly, *V. falcata* associates with a

371   group of *Ceratobasidium* fungi for seed germination.

372   Although amplicon sequencing results are not thought to directly reflect fungal community

373   outside samples (i.e., bark surface), the results suggest that the growing substrate does not

374   necessarily provide suitable conditions for OM establishment in epiphytic orchids. Based on

375   the information obtained from PCoA, it was shown that the fungal community in seeds, young,

376   and adult plants were similar with slight differences. Ascomycetous fungal classes, such as

377   Sordariomycetes, Dothideomycetes, and Leotiomycetes frequently occur in all samples, and

378   most of the members are known to be saprobic or parasitic in several habitats, including tree

379   surface where epiphytic orchids coexist (Schoch et al. 2009; Herrera et al. 2010). Seeds

380   landing on bark become the potential hosts of these fungi, especially for *Rhizoctonia*-like

381   fungi, present on the same site. Although it is unknown whether the proportion of

382   ascomycetous and *Rhizoctonia*-like fungi on *D. kaki* bark is similar to that inside *V. falcata*

383   seeds, in the end, ascomycetous fungi will be dominant in the seeds. Even if compatible

384   *Rhizoctonia*-like fungus is present inside the seeds, ascomycetous fungi could encompass the

385   seeds even before germination occurs. Severe infection of *Pyrenochaetopsis* and *Fusarium,*

386   which were isolated from healthy roots upon inoculation with these fungi, indicates that the

387   presence of ascomycetous fungi is a potential hinderance for *V. falcata* germination. As

388   with any endophytic relationship, there is a balanced state between endophyte and roots

389   where the endophyte inhabits within the root without damage to the root. However, when

390   the endophyte was grown on nutrient rich media, it may exhibit virulence against the host

391   (Sarsaiya et al. 2020). In this study, *V. falcata* seeds dispersed on the substrate was

392   vulnerable to *Pyrenochaetopsis* and *Fusarium*.

393   In the case of *Rhizoctonia*-like fungi, sequence reads in *Serendipita* OTUs were high in

394   seeds, but they much lower in young and adult roots. Conversely, little reads in *Tulasnella*

395   were found in seeds, but its occurrence increases in young and adult roots. The occurrence of

396   *Serendipita* OTUs compared to that of *Ceratobasidium* and *Tulasnella* in seeds indicates the

397   shifting of *Rhizoctonia*-like fungi preference during development but may not necessarily

398   reflect the actual OM association. If *Serendipita* is the OMF of *V. falcata*, seeds in baiting

399   samples should have germinated. Although the number of OTU sequences for *Serendipita*,

400   *Tulasnella*, and *Ceratobasidium* were different at each developmental stage as mentioned, the

401   function of these Rhizoctonia-like fungi is difficult to be speculated based only on the current

402   data and needs to be further investigated.

403   Among all fungi isolated from root sections, *Ceratobasidium* sp. BI and *C*. sp. DE from

404   young and adult plant roots were confirmed to associate with *V. falcata* due to their capability

405   to propagate seed germination. Interestingly, another strain *Ceratobasidium sp.* TA2 isolated

406   from an epiphytic orchid *Taeniophyllum glandulosum* in Shizuoka Prefecture (Rammitsu et al.

407   2019) induced better germination results. These three *Ceratobasidium* strains formed a similar

408   clade in the phylogenetic analysis. Therefore, it is suggested that *V. falcata* associates with a

409   narrow range of *Ceratobasidium* in seed germination. Associating with various fungi is

410 advantageous if the OMF occurrence is sporadic, which allows the orchid to readily develop

411 with any compatible fungus available on each growing site (Xing et al. 2019). Generally, it is

412 accepted that orchids with high mycorrhizal specificity are most likely to be rare due to high

413 dependency on OMF distribution in their natural habitats. In the case of *V. falcata*, its

414 distributions were constricted from central to southern Japan with various types of

415 phorophytes (Suetsugu et al. 2015; Rammitsu et al. 2019, 2021). Accordingly, *V. falcata* has

416 high phenotypic variation even for wild plants across Japan, causing such extensive

417 association to be beneficial to the plant for distribution.

418 We propose that the partitioning of OMF and ascomycetous fungi protects the mycorrhizal

419 root. In this study, ascomycetous fungi mainly detected in *V. falcata* roots were

420 Sordariomycetes, Dothideomycetes, and Leotiomycetes, commonly known as saprobes and

421 pathogens on tree bark (Naranjo-Ortiz and Gabaldón 2019). Primarily based on their saprobic

422 nature, it is plausible that these fungi mainly colonize *D. kaki* bark, and through the orchid

423 root-bark interface, these fungi further penetrate velamen. Although OMF can penetrate into

424 cortical cells, invasion of the ascomycetous fungi is inhibited by exodermis, thus

425 accumulating them inside velamen. Orchid roots typically contain exodermis with

426 lignification of the tangential walls and smaller, non-lignified passage cells that allow OMF to

427 penetrate the cortical cells (Esnault et al. 1994). It is also reported that the passage cell is

428 related to OMF colonization; that is, the root part with denser passage cells has more OMF

429 colonization (Chomicki et al. 2014). Based on these concepts, we also confirmed that passage

430 cells exist in both root surfaces, those attached to bark and those exposed to the air, and the

431 lower part attached to bark had dense passage cells, which was related to higher mycorrhizal

432 colonization in this part. While passage cells are constantly available for OMF to infiltrate,

433 the upper parts of the root mostly remain uncolonized. The exact explanations for this finding

19

434 are still lacking, but we suggest that chemical (deposition of phenolics, etc.) or environmental

435 (light exposure, etc.) factors might be included. Further studies on how internal and external

436 factors affect epiphytic root colonization by fungi are required to elaborate on this

437 phenomenon.

438

439 **Conclusions**

440 To sum up, *V. falcata's* fungal community structure is similar across growth development.

441 Ascomycota was the dominant phylum, while the others were found in a smaller amount,

442 even for *Rhizoctonia*-like fungi (Fig. 8). It was also confirmed that seeds of *V. falcata*

443 germinated in symbioses with *Ceratobasidium* isolated from its roots and another strain

444 isolated from another orchid. We also propose that the innate regulation of fungal entry also

445 causes this balanced fungal community and partitioning of ascomycetes as well as OMF.

446 Therefore, further studies on how root balances fungal colonization are required to decipher

447 this partitioning mechanism in *V. falcata* or any other epiphytic orchids.

448

449 **Data Accessibility**

450 The raw sequence reads have been deposited into the DNA Data Bank of Japan (DDBJ)

451 Sequence Read Archive database under the accession number DRA012420 for ITS1 and

452 DRA012422 for ITS2. OTU sequences were registered as LC602782 - LC602786 for

453 *Ceratobasidium,* LC602787 - LC602792 for *Serendipita*, and LC602793 - LC602794 for

454 *Tulasnella.* ITS sequences of isolated *Ceratobasidium* were registered as LC600231for BI-

455 103P and LC600232 for DE-52P.

456

457 **Author Contributions**

458   GCP, CM, MY, and HK designed the experiments; GCP and IN performed the experiments

459   and analyzed the sequencing data; GCP, CM, MY, and HK wrote the manuscript. All authors

460   approved the final manuscript.

461

462   **Acknowledgments**

469

470   **Conflict of interest**

471   The authors declare no competing interests.

472

References

Almeida PRM, van den Berg C, Góes-Neto A (2014) *Epulorhiza amonilioides* sp. nov.: a new anamorphic species of orchid mycorrhiza from Brazil. Neodiversity 7:1–10. https://doi.org/10.13102/neod.71.1

Arditti J, Ghani AKA (2000) Numerical and physical properties of orchid seeds and their biological implications. New Phytologist 145:367–421. https://doi.org/10.1046/j.1469-8137.2000.00587.x

Barthlott W, Große-Veldmann B, Korotkova N (2014) Orchid seed diversity: A scanning electron microscopy survey. Englera, Berlin. ISBN: 9783921800928

Bolyen E, Rideout JR, Dillon MR, et al (2019) Reproducible, interactive, scalable and extensible microbiome data science using QIIME 2. Nature Biotechnology 37:852–857. https://doi.org/10.1038/s41587-019-0209-9

Carlsward BS, Whitten WM, Williams NH, Bytebier B (2006) Molecular phylogenetics of Vandeae (Orchidaceae) and the evolution of leaflessness. American Journal of Botany 93:770–786. https://doi.org/10.3732/ajb.93.5.770

Chomicki G, Bidel LPR, Jay-Allemand C (2014) Exodermis structure controls fungal invasion in the leafless epiphytic orchid *Dendrophylax lindenii* (Lindl.) Benth. ex Rolfe. Flora 209:88–94. https://doi.org/10.1016/j.flora.2014.01.001

Clarke KR (1993) Non-parametric multivariate analysis of changes in community structure. Australian Journal of Ecology 18:117–143. https://doi.org 10.1111/j.1442-9993.1993.tb00438.x

22

494   Esnault A-L, Masuhara G, McGee PA (1994) Involvement of exodermal passage cells in

495   mycorrhizal infection of some orchids. Mycological Research 98:672–676.

496   https://doi.org/10.1016/S0953-7562(09)80415-2

497   Freitas EFS, da Silva M, Cruz E da S, et al (2020) Diversity of mycorrhizal *Tulasnella*

498   associated with epiphytic and rupicolous orchids from the Brazilian Atlantic Forest,

499   including four new species. Scientific Reports 10:7069. https://doi.org/10.1038/s41598-

500   020-63885-w

501   Gange AC, Bower E, Stagg PG, et al (1999) A comparison of visualization techniques for

502   recording arbuscular mycorrhizal colonization. New Phytologist 142: 123-132.

503   https://doi.org /10.1046/j.1469-8137.1999.00371.x

504   Guimarães FAR, Pereira MC, Felício C da S, et al (2013) Symbiotic propagation of seedlings

505   of *Cyrtopodium glutiniferum* Raddi (Orchidaceae). Acta Botanica Brasilica 27:590–596.

506   https://doi.org/10.1590/S0102-33062013000300016

507   Hannon GJ (2010) FASTX-Toolkit.

508   Herrera P, Suárez JP, Kottke I (2010) Orchids keep the ascomycetes outside: a highly diverse

509   group of ascomycetes colonizing the velamen of epiphytic orchids from a tropical

510   mountain rainforest in Southern Ecuador. Mycology 1:262–268.

511   https://doi.org/10.1080/21501203.2010.526645

512   Hoang NH, Kane ME, Radcliffe EN, et al (2017) Comparative seed germination and seedling

513   development of the ghost orchid, *Dendrophylax lindenii* (Orchidaceae), and molecular

514   identification of its mycorrhizal fungus from South Florida. Annals of Botany 119:379–

515   393. https://doi.org/10.1093/aob/mcw220

23

516   Ihrmark K, Bödeker ITM, Cruz-Martinez K, et al (2012) New primers to amplify the fungal

517   ITS2 region - evaluation by 454-sequencing of artificial and natural communities. FEMS

518   Microbiology Ecology 82:666–677. https://doi.org/10.1111/j.1574-6941.2012.01437.x

519   Inglis PW, Marilia de Castro RP, Resende L V., Grattapaglia D (2018) Fast and inexpensive

520   protocols for consistent extraction of high quality DNA and RNA from challenging plant

521   and fungal samples for high-throughput SNP genotyping and sequencing applications.

522   PLoS ONE 13:1–14. https://doi.org/10.1371/journal.pone.0206085

523   Joshi N, Fass JN (2011) Sickle: A sliding-window, adaptive, quality-based trimming tool for

524   FastQ files (Version 1.33). Available at https://github.com/najoshi/sickle.

525   Kassambara A (2018) ggpubr: "ggplot2" Based Publication Ready Plots. R package version

526   0.2. Available at https://CRAN.R-project.org/package=ggpubr.

527   Kendon JP, Yokoya K, Zettler LW, et al (2020) Recovery of mycorrhizal fungi from wild

528   collected protocorms of Madagascan endemic orchid *Aerangis ellisii* (B.S. Williams)

529   Schltr. and their use in seed germination in vitro. Mycorrhiza 30:567-576.

530   https://doi.org/10.1007/s00572-020-00971-x

531   Kuga Y, Sakamoto N, Yurimoto H (2014) Stable isotope cellular imaging reveals that both

532   live and degenerating fungal pelotons transfer carbon and nitrogen to orchid protocorms.

533   New Phytologist 202:594–605. https://doi.org/10.1111/nph.12700

534   Magoč T, Salzberg SL (2011) FLASH: Fast length adjustment of short reads to improve

535   genome assemblies. Bioinformatics 27:2957–2963.

536   https://doi.org/10.1093/bioinformatics/btr507

537   Moore RM, Harrison AO, McAllister SM, et al (2020) Iroki: automatic customization and

538   visualization of phylogenetic trees. PeerJ 8:e8584. https://doi.org/10.7717/peerj.8584

539   Mújica EB, Mably JJ, Skarha SM, et al (2018) A comparision of ghost orchid (*Dendrophylax*

540   *lindenii*) habitats in Florida and Cuba, with particular reference to seedling recruitment

541   and mycorrhizal fungi. Botanical Journal of the Linnean Society 186:572–586.

542   https://doi.org/10.1093/botlinnean/box106

543   Naranjo-Ortiz MA, Gabaldón T (2019) Fungal evolution: major ecological adaptations and

544   evolutionary transitions. Biological Reviews 94:1443–1476.

545   https://doi.org/10.1111/brv.12510

546   Nilsson RH, Larsson KH, Taylor AFS, et al (2019) The UNITE database for molecular

547   identification of fungi: Handling dark taxa and parallel taxonomic classifications.

548   Nucleic Acids Research 47:D259–D264. https://doi.org/10.1093/nar/gky1022

549   Oberwinkler F, Riess K, Bauer R, et al (2013) Taxonomic re-evaluation of the

550   *Ceratobasidium-Rhizoctonia* complex and *Rhizoctonia butinii*, a new species attacking

551   spruce. Mycological Progress 12:763–776. https://doi.org/10.1007/s11557-013-0936-0

552   Ogle DH, Wheeler P, Dinno A (2021) FSA: Fisheries Stock Analysis. R package version

553   0.9.1.9000. Available at https://github.com/droglenc/FSA.

554   Ogoshi A (1975) Studies on the anastomosis groups of *Rhizoctonia solani* Kühn. Bull Natl

555   Inst, Agrie Sci Ser C 9:198–203

556   Oksanen J, Legendre P, O'Hara B, et al (2007) The vegan package. Community ecology

557   package 10:631–637. Available at http://vegan.r-forge.r-project.org/

558   Otero JT, Ackerman JD, Bayman P (2002) Diversity and host specificity of endophytic

559   *Rhizoctonia*-like fungi from tropical orchids. American Journal of Botany 89:1852–1858.

560   https://doi.org/10.3732/ajb.89.11.1852

561   Pujasatria GC, Miura C, Kaminaka H (2020) In vitro symbiotic germination: A revitalized

562   heuristic approach for orchid species conservation. Plants 9:1–15.

563   https://doi.org/10.3390/plants9121742

564   Rachanarin C, Suwannarach N, Kumla J, et al (2018) A new endophytic fungus, *Tulasnella*

565   *phuhinrongklaensis* (Cantharellales, Basidiomycota) isolated from roots of the terrestrial

566   orchid, *Phalaenopsis pulcherrima*. Phytotaxa 374:99–109.

567   https://doi.org/10.11646/phytotaxa.374.2.1

568   Rammitsu K, Kajita T, Imai R, Ogura-Tsujita Y (2021) Strong primer bias for Tulasnellaceae

569   fungi in metabarcoding: Specific primers improve the characterization of the mycorrhizal

570   communities of epiphytic orchids. Mycoscience 62:1–17.

571   https://doi.org/10.47371/mycosci.2021.06.005

572   Rammitsu K, Yagame T, Yamashita Y, et al (2019) A leafless epiphytic orchid,

573   *Taeniophyllum glandulosum* Blume (Orchidaceae), is specifically associated with the

574   Ceratobasidiaceae family of basidiomycetous fungi. Mycorrhiza 29:159–166.

575   https://doi.org/10.1007/s00572-019-00881-7

576   Rasmussen HN, Dixon KW, Jersáková J, Těšitelová T (2015) Germination and seedling

577   establishment in orchids: A complex of requirements. Annals of Botany 116:391–402.

578   https://doi.org/10.1093/aob/mcv087

579   Rasmussen HN, Rasmussen FN (2018) The epiphytic habitat on a living host: Reflections on

580   the orchid-tree relationship. Botanical Journal of the Linnean Society 186:456–472.

581   https://doi.org/10.1093/botlinnean/box085

582   Riess K, Oberwinkler F, Bauer R, Garnica S (2014) Communities of endophytic Sebacinales

583   associated with roots of herbaceous plants in agricultural and grassland ecosystems are

584   dominated by *Serendipita herbamans* sp. nov. PLoS ONE 9: e94676.

585   https://doi.org/10.1371/journal.pone.0094676

586   Sarsaiya S, Jain A, Jia Q, et al (2020) Molecular identification of endophytic fungi and their

587   pathogenicity evaluation against *Dendrobium nobile* and *Dendrobium officinale.*

588   International Journal of Molecular Sciences 21:1–16.

589   https://doi.org/10.3390/ijms21010316

590   Schoch CL, Sung GH, López-Giráldez F, et al (2009) The Ascomycota tree of life: A phylum-

591   wide phylogeny clarifies the origin and evolution of fundamental reproductive and

592   ecological traits. Systematic Biology 58:224–239. https://doi.org/10.1093/sysbio/syp020

593   Singh US, Kumar J (1991) Staining of nuclei in fungi by ethidium bromide. Biotechnic and

594   Histochemistry 66:266–268. https://doi.org/10.3109/10520299109109984

595   Suetsugu K, Tanaka K, Okuyama Y, Yukawa T (2015) Potential pollinator of *Vanda falcata*

596   (Orchidaceae): *Theretra* (Lepidoptera: Sphingidae) hawkmoths are visitors of long

597   spurred orchid. European Journal of Entomology 112:393–397.

598   https://doi.org/10.14411/eje.2015.031

27

599   Taylor DL, McCormick MK (2008) Internal transcribed spacer primers and sequences for

600   improved characterization of basidiomycetous orchid mycorrhizas. New Phytologist

601   177:1020–1033. https://doi.org/10.1111/j.1469-8137.2007.02320.x

602   Toju H, Tanabe AS, Yamamoto S, Sato H (2012) High-coverage ITS primers for the DNA-

603   based identification of ascomycetes and basidiomycetes in environmental samples. PLoS

604   ONE 7: e40863. https://doi.org/10.1371/journal.pone.0040863

605   Warcup JH, Talbot PHB (1980) Perfect States of Rhizoctonias Associated With Orchids. Iii.

606   New Phytologist 86:267–272. https://doi.org/10.1111/j.1469-8137.1980.tb00787.x

607   Weiß M, Waller F, Zuccaro A, Selosse MA (2016) Sebacinales - one thousand and one

608   interactions with land plants. New Phytologist 211:20–40.

609   https://doi.org/10.1111/nph.13977

610   Xing X, Jacquemyn H, Gai X, et al (2019) The impact of life form on the architecture of

611   orchid mycorrhizal networks in tropical forest. Oikos 128:1254–1264.

612   https://doi.org/10.1111/oik.06363

613   Yang RH, Su JH, Shang JJ, et al (2018) Evaluation of the ribosomal DNA internal transcribed

614   spacer (ITS), specifically ITS1 and ITS2, for the analysis of fungal diversity by deep

615   sequencing. PLoS ONE 13:1–17. https://doi.org/10.1371/journal.pone.0206428

616   Yeh CM, Chung KM, Liang CK, Tsai WC (2019) New insights into the symbiotic

617   relationship between orchids and fungi. Applied Sciences 9:1–14.

618   https://doi.org/10.3390/app9030585

619   Yukawa T, Ogura-Tsujita Y, Shefferson RP, Yokoyama J (2009) Mycorrhizal diversity in

620   *Apostasia* (Orchidaceae)indicates the origin and evolution of orchid mycorrhiza.

621   American Journal of Botany 96:1997–2009. https://doi.org/10.3732/ajb.0900101

622   Zettler LW, Corey LL, Jacks AL, et al (2013) *Tulasnella irregularis* (Basidiomycota:

623   Tulasnellaceae) from roots of *Encyclia tampensis* in South Florida, and confirmation of

624   its mycorrhizal significance through symbiotic seed germination. Lankesteriana 13:119–

625   128. https://doi.org/10.15517/lank.v0i0.11552

626   Zettler LW, Poulter SB, McDonald KI, Stewart SL (2007) Conservation-driven propagation

627   of an epiphytic orchid (*Epidendrum nocturnum*) with a mycorrhizal fungus. HortScience

628   42: 135-139. https://doi.org/10.21273/hortsci.42.1.135

629   Zhang Y, Crous PW, Schoch CL, Hyde KD (2012) Pleosporales. Fungal Diversity 53:1–221.

630   https://doi.org/10.1007/s13225-011-0117-x

631

632

Figure legends

Fig. 1. Plant samples. A) Location of Mie Prefecture, Kihoku Town, and Suzuka City (green) inside Japan. B) *Vanda falcata* young plant example. C) Adult plants with old, drying inflorescences. D) Colonized root parts conspicuously turned yellow upon orchid mycorrhizal fungi (OMF) colonization (arrowheads). E) OMF mostly colonizes the root part that attaches to the bark. Bar = 1-mm.

Fig. 2. Beta diversity of the fungi in *Vanda falcata* based on the ITS1 and ITS2 sequences. Principal coordinate analysis (PCoA) plots of ITS1 (A) and ITS2 (B) based on Bray-Curtis distance showing a composition of fungal community structure in all samples, e.g., seeds from seed baiting (SB, red), young plant roots (YR, green), and adult plant roots (AR, blue). R-value was calculated using ANOSIM ($p < 0.05$).

Fig. 3. *Rhizoctonia*-like fungal OTUs inferred from amplicon sequencing results. A) Heat map diagram showing *Rhizoctonia*-like fungi OTUs present in seed (SB), seedling (Y1-3), and adult (A1-4) root samples. B) Maximum likelihood (ML) phylogenetic tree of OTUs assigned to each order (colored branches)–Cantharellales (chartreuse) and Sebacinales (light blue)–and family (arcs): Ceratobasidiaceae (green), Serendipitaceae (blue), Sebacinaceae (light blue), and Tulasnellaceae (yellow). Only bootstrap numbers above 80% (dotted nodes) are shown. *Clavulina caespitosa, Craterellus atratoides,* and *Craterellus indicus* are used as outgroups from Cantharellales.

Fig. 4. Colonization of ascomycetous and orchid mycorrhizal fungi (OMF) inside roots. A) Conidia of *Lasiodiplodia* (L) and unidentified Pleosporales (P) on the epidermis. B) OMF

30

657 hyphae (arrowheads) infiltrating the cortical cells (Co) through velamen (VR) and passage

658 cell (PC) of exodermis (Ex). Bar = 40 μm. C) Localization of exodermal passage cells in the

659 upper, side, and lower parts of root (left), and those colonized by OMF (right). Different

660 letters represent significant difference by Tukey's test at p < 0.05.

661

662 **Fig. 5.** *In vitro* germination assay results. *Vanda falcata* seeds were inoculated with eleven

663 *Rhizoctonia*-like fungi, including those isolated in this study (BI-103P and DE-52P). Boxplots

664 showing growth index (A) and symbiotic cell count (B) after eight weeks. Different letters

665 represent significant difference by Dunn's test at p < 0.05.

666

667 **Fig. 6.** Maximum likelihood phylogenetic tree of *Ceratobasidium* strains, including those

668 inducing seed germination of *Vanda falcata* (red) and other isolated strains (blue). Dotted

669 nodes indicate a bootstrap number of 80% or higher. The clade containing strains with the

670 best germination output is shown in chartreuse branches. Adjacent boxes indicate the

671 nutritional mode of each species, i.e., plant-pathogen (red), saprobe (yellow), orchid

672 mycorrhizal fungus (green), and lichen-forming (blue). *Rhizoctonia solani* strains are used as

673 an outgroup (red branches).

674

675 **Fig. 7.** Infected *Vanda falcata* seeds upon inoculation with pathogenic ascomycetous fungi

676 isolated from *V. falcata* roots. A) Seeds infected with *Pyrenochaetopsis*. Black, swollen seed

677 (arrow) was filled with pycnidium. (B) Seed colonized by *Fusarium*. Although inconspicuous,

678 the seed starts to degrade.

679

680 **Fig. 8**. Inner fungal community composition in *Vanda falcata*. Along with growth and

681 development (i.e., from seed germination to reproductive stage), despite an increase in size

682 and trophic mode, the inner fungal community has a similar structure with Ascomycota as the

683 dominant phylum, followed by Basidiomycota. Even for Basidiomycota, *Rhizoctonia*-like

684 fungi abundance is less than half compared to other genera. Among all *Rhizoctonia*-like fungi,

685 *Ceratobasidium* is the OMF of *V. falcata* based on germination assay results, thus correlating

686 with its higher portion. Additionally, only *Rhizoctonia*-like fungus colonizes cortical cells

687 through exodermal passage cells.

688

689   **Table 1.** *Rhizoctonia*-like fungi used for *Vanda falcata* seed symbiotic germination

Treatment	Species name	Strain no.	Source	
			Host plant	Location
C.gra53	*Ceratobasidium gramineum*	MAFF235853	*Agrostis sp.* * **	Japan
C.sp.87	*Ceratobasidium sp.*	MAFF244587	*Dactylorhiza aristata*	Japan
C.sp.BI	*Ceratobasidium sp.*	N/A	this study	Japan
C.sp.DE	*Ceratobasidium sp.*	N/A	this study	Japan
C.sp.TA1	*Ceratobasidium sp.*	NBRC109234	*Taeniophyllum glandulosum*	Japan
C.sp.TA2	*Ceratobasidium sp.*	NBRC109235	*Taeniophyllum glandulosum*	Japan
S.ind27	*Serendipita indica*	ATCC DSM11827	*Prosopis juliflora* and *Zizyphus nummularia* * ***	India
S.ver30	*Serendipita vermifera*	MAFF305830	*Cyrtostylis reniformis*	Australia
T.asy08	*Tulasnella asymmetrica*	MAFF305808	*Thelymitra epipactoides*	Australia
T.cal05	*Tulasnella calospora*	MAFF305805	unspecified	Australia
T.irr96	*Tulasnella irregularis*	JCM9996	*Dendrobium dicuphum*	Australia

* Non-orchidaceous plants, ** isolated as pathogen, *** isolated as endophyte

690

691 **Table 2.** Seed germination stage morphological descriptions

Stage	Description
0	No response
1	Imbibition, OMF starts to colonize
2	Swelling, testa rupture, formation of rhizoids
3	Formation of shoot primordium
4	Formation of first crest
5	Formation of first leaf

692

693 **Table 3.** Isolated fungi from *Vanda falcata* seedling and adult plant roots

Isolate	Source sample	Closest match in Genbank	Similarity
BI-103P	Young root	AB507066.1 uncultured Ceratobasidiaceae from *Sedirea japonica* (Miyazaki Prefecture, Japan)	97.74%
DE-52P	Adult plant root	AB507066.1 uncultured Ceratobasidiaceae from *Sedirea japonica* (Miyazaki Prefecture, Japan)	98.79%
MI-3	Young root	NR_155625.1 *Parateratosphaeria karinae* holotype CBS128774 (South Africa)	84.20%
MI-4	Young root	NR_153559.1 *Atrocalyx bambusae* holotype MFLU 11-0150 (Thailand)	97.25%
MI-5	Young root	NR_159064.1 *Subulicystidium harpagum* isotype KAS L 1726a (Réunion Island)	89.26%
NE-4	Adult plant root	NR_160059.1 *Pyrenochaetopsis microspora* type material CBS 102876 (Montenegro)	99.81%
NE-5	Adult plant root	NR_137617.1 *Fusicolla violacea* holotype CBS:634.76 (Iran)	80.92%

694

Fig. 1

A

Mie Prefecture

Suzuka

Kihoku

B

C

D

E

OMF

Bark

Fig. 2

A ITS1 (R-value = 0.3913, sig. = 0.0419)
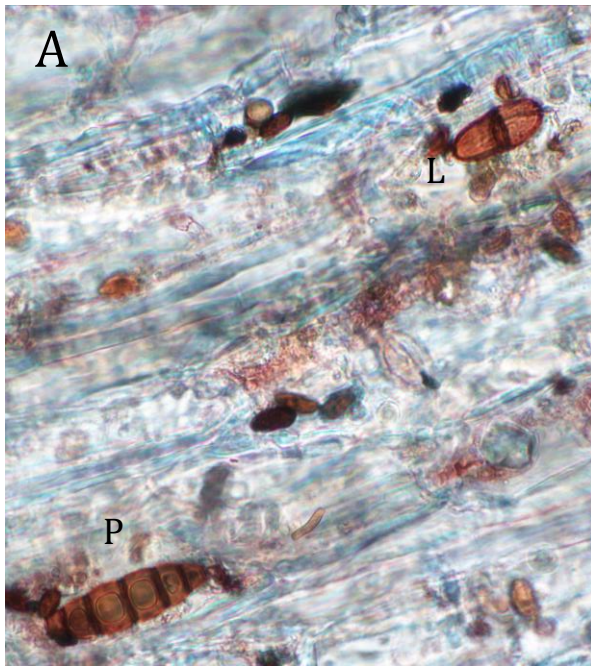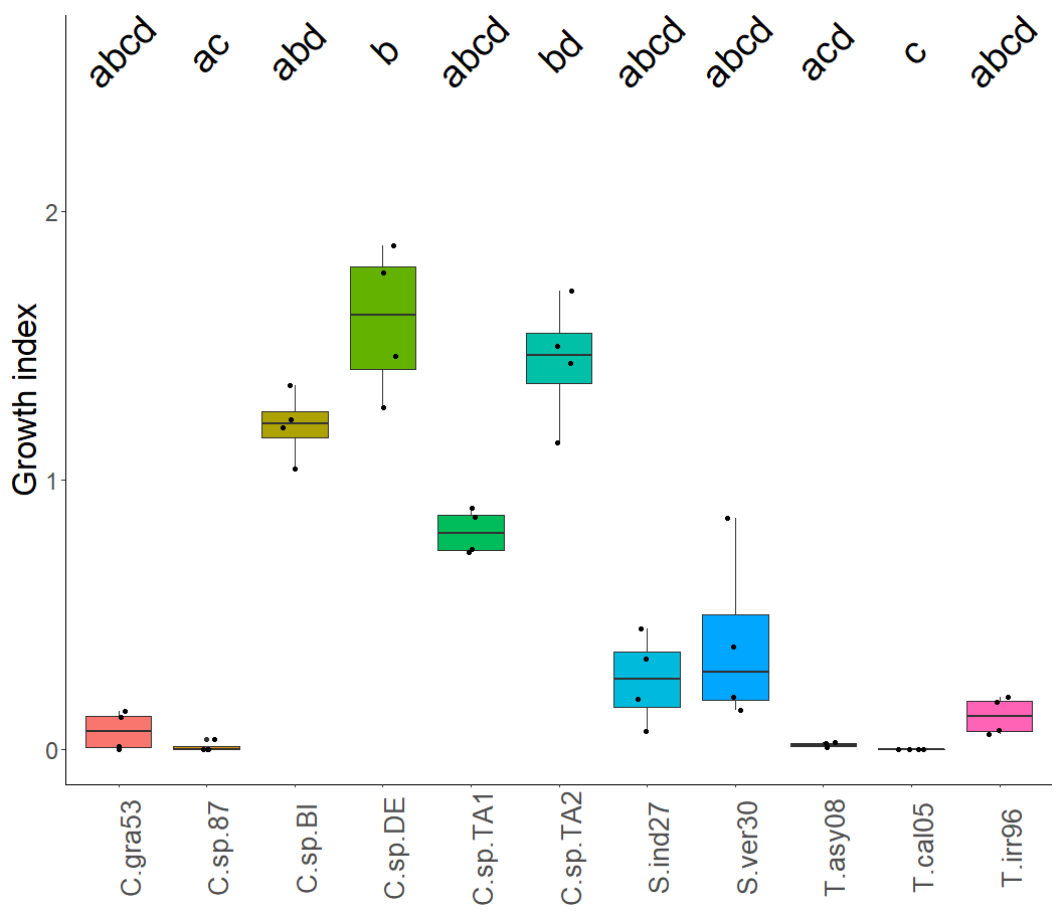
B ITS2 (R-value = 0.2047, sig. = 0.1965)

Fig. 3

Fig. 4

Fig. 5   A

Fig. 6

Fig. 7

Fig. 8